

Automatic Slide-Loader Fluorescence Microscope for Discriminative Enumeration of Seafloor Life

by Yuki Morono and Fumio Inagaki

doi:10.2204/iodp.sd.9.05.2010

Introduction

The marine subsurface environment is considered the potentially largest ecosystem on Earth, harboring one-tenth of all living biota (Whitman et al., 1998) and comprising diverse microbial components (Inagaki et al., 2003, 2006; Teske, 2006; Inagaki and Nakagawa, 2008). In deep marine sediments, the discrimination of life is significantly more difficult than in surface sediments and terrestrial soils because buried cells generally have extremely low metabolic activities (D'Hondt et al., 2002, 2004), and a highly consolidated sediment matrix produces auto-fluorescence from diatomaceous spicules and other mineral particles (Kallmeyer et al., 2008). The cell abundance in marine subsurface sediments has conventionally been evaluated by acridine orange direct count (AODC; Cragg et al., 1995; Parkes et al., 2000) down to 1613 meters below the seafloor (mbsf) (Roussel et al., 2008). Since the cell-derived AO signals often fade out in a short exposure time, recognizing and counting cells require special training. Hence, such efforts to enumerate AO-stained cells from the seafloor on photographic images have been difficult, and a verification of counts by other methods has been impossible. In addition, providing mean statistical values from low biomass sedimentary habitats has been complicated by physical and time limitations, yet these habitats are considered critical for understanding the Earth's biosphere close to the limits of habitable zones (Hoehler, 2004; D'Hondt et al., 2007).

Here we report recent developments on the automatic cell count system based on our recently published new cell detection and enumeration method that discriminates the SYBR Green I (SYBR I)-stained cells from the background fluorescent signals, called SYBR-SPAM (SYBR-Stainable Particulated Matter; Morono et al., 2009). We integrated an automatic slide loader and an LED light-camera monitoring system for high-throughput and high-resolution counting operation.

Principle of Discriminative Detection

SYBR-I or SYBR-II has been considered a more effective fluorescent dye for cell enumeration in sediments than AO due to its higher fluorescent intensity and sensitivity to nucleic acids (Weinbauer et al., 1998; Lunau et al., 2005;

Engelen et al., 2008). However, we found non-autofluorescent SYBR-I-stainable particulate matter (SYBR-SPAM) in heat-sterilized control sediments treated at 450°C for 3 hours (Morono et al., 2009). We also found that when SYBR-I bound to SYBR-SPAM the SYBR-I spectra shifted to longer wavelengths (Fig. 1A), and that the spectra can be distinguished from cell-derived green fluorescence under the observation of a long-pass filter of cut-off wavelength 510 nm (Fig. 1B). To discriminate the cell-derived fluorescent signal more precisely, we obtained microscopic images using band-pass filters at 528/38 and 617/73 nm (center wavelength/bandwidth) that separated the green and red components of SYBR-I fluorescence (Fig. 1C, D). We divided the fluorescent intensity of green by that of the red images to obtain relative intensity profiles of green/red fluorescence, in which cell-derived fluorescence was successfully discriminated as bright signals, whereas SYBR-SPAM and other background signals were entirely eliminated (Fig. 1E).

Sample Preparation Protocol

A standard sample preparation scheme is shown in Fig. 2. Fifty microliters of sediment slurry (10% [v/v] sediment in ethanol-PBS solution) fixed in 2% paraformaldehyde is mixed with 850 µL of 3% [wt/v] NaCl solution and sonicated at 20 W for 1 min on ice using an ultrasonic homogenizer (Model UH-50, SMT Co. Ltd., Tokyo). The sonicate is then mixed with 100 µL of 10% [wt/v] hydrofluoric acid (HF) and incubated for 20 min at room temperature. This HF treatment has been shown to effectively decrease the number of SYBR-SPAM especially in shallow seafloor sediments, while intracellular DNA is negligibly affected (Morono et al., 2009). Then, up to 700 µL of the mixture is directly filtered through a 0.22 µm-pore size black polycarbonate membrane without centrifugation. The final sediment volumes on the filter are up to $3.5 \times 10^{-3} \text{ cm}^3$. To eliminate potential carbonate particles and/or precipitates, the membrane is treated with 1 mL of 0.1 M HCl for 5 min on the filtration device. The membrane is then washed with 5 mL of TE buffer (10 mM Tris-HCl, 1.0 mM EDTA, pH 8.0), and roughly 2×10^8 fluorescence microsphere beads (Fluoresbrite Bright Blue Carboxylate Microspheres [BB beads], 0.5 µm, Polysciences, Inc., Warrington, Pa.) are used for focus adjustment (Morono et al., 2009). After air drying, one-fourth of the membrane is placed on the filtration device again, then stained with SYBR-I staining solution (1/40 [v/v] SYBR-I in TE buffer). The stained filter is finally mounted on a glass microscope

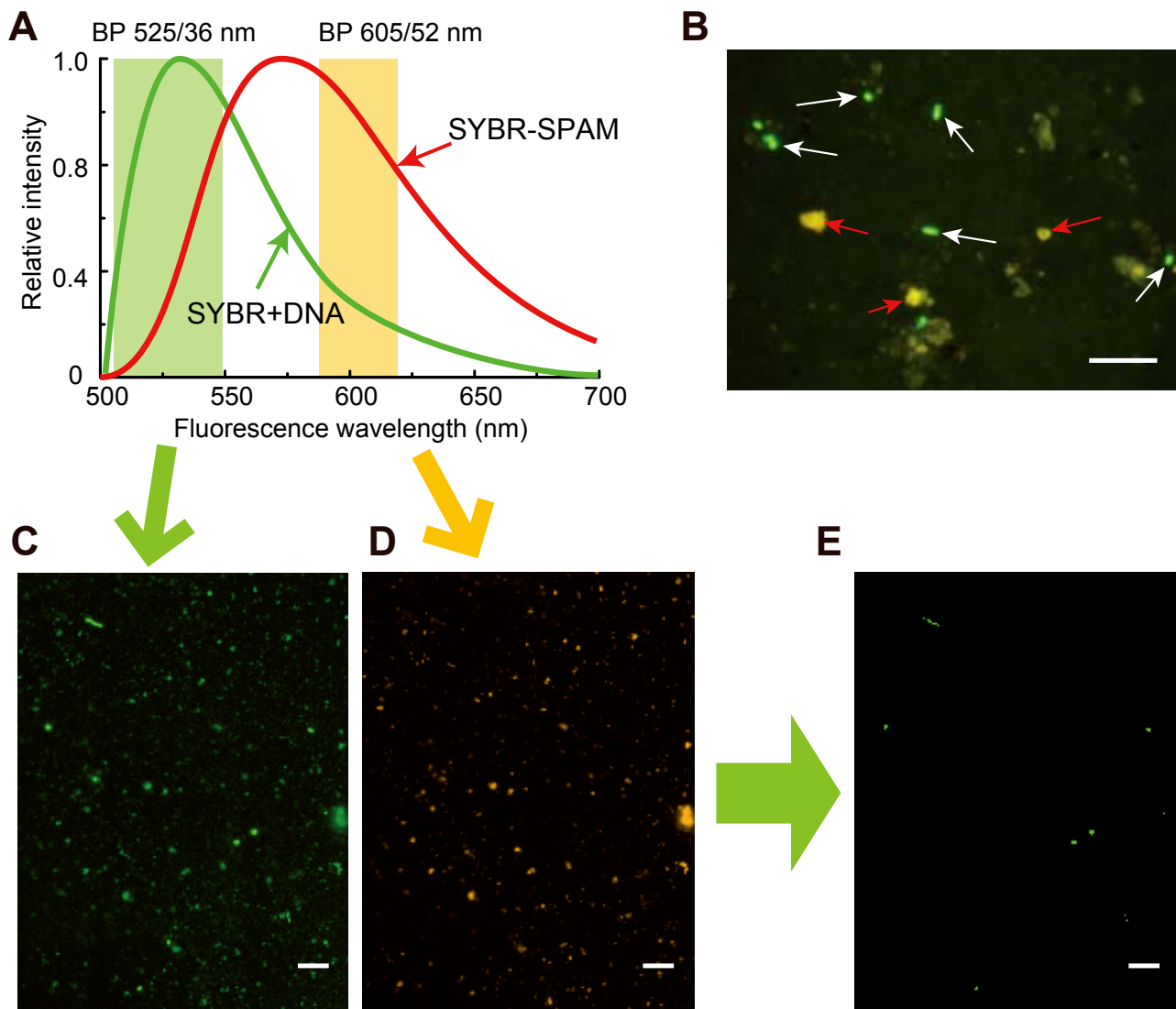


Figure 1. Difference of SYBR-I fluorescence spectrum with intracellular DNA or SYBR-SPAM, and discrimination of cell-derived SYBR Green I fluorescence from background signals using image analysis. [A] Spectrum patterns show "red shift" of SYBR-I fluorescence. When SYBR-I binds to SYBR-SPAM (red line), fluorescence spectra shift to longer wavelengths than SYBR-DNA complex (green line). Green and orange shaded areas show the wavelength range of 525/36 and 605/52 (nm of center wavelength/bandwidth) band-pass filters, respectively. [B] Examples of fluorescence-producing cellular and non-cellular objects stained with SYBR-I. Red arrows, yellowish SYBR-SPAM. White arrows, green *E. coli* cells. The image was obtained using a long-pass filter of cut-off wavelength 510 nm. [C to E] Image analysis to distinguish cell-derived SYBR-I signals from SYBR-SPAM in natural marine sediments (core 1H-1 of Site C0006 Hole E in the Integrated Ocean Drilling Program Exp. 316). Fluorescence microscopic images taken using band-pass filters of 525/36 [C] and 605/52 [D]. Relative intensity profiles of green/red fluorescence [E] show only cell-derived fluorescence signals without background fluorescence. Bars: 10 μ m.

slide with 3–5 μ L of mounting solution (1:2 mixture of VECTASHIELD mounting medium H-1000 and TE buffer).

The Slide Handler-Equipped Automatic Fluorescence Microscope System

The images are automatically acquired with a fluorescent microscope system (Fig. 3A) that consists of a basic microscope (BX-51, Olympus), an automatic slide handler (LEP Slide Handler System, Ludl Electric Products, Ltd.), illumination with LED Array Modules (LAMs) of 400 nm and 490 nm (precisExcite, CoolLED, Ltd.), an emission filter wheel (Ludl Electric Products, Ltd.), and a cooled CCD

camera (ORCA-AG, Hamamatsu Photonics K.K.). All units are software controlled (MetaMorph 7.5, Molecular Devices). Up to 50 slides of samples can be set in two magazines of the slide handler (Fig. 3B). To keep the sample in good condition for a long time (depending on the scanning area but at least 30 min per sample, i.e., 25 h duration to process all 50 slides), the whole system is put in a dark cooled (15°C) chamber. In addition, we also installed a digital camera to monitor the system without opening the door of the chamber (Fig. 3C, D). LED illumination allows for (i) an instant on/off switch and wavelength change without damage to the lamp source, (ii) a prolonged lifetime in comparison to mercury lamps, and (iii) negligible heating during operation.

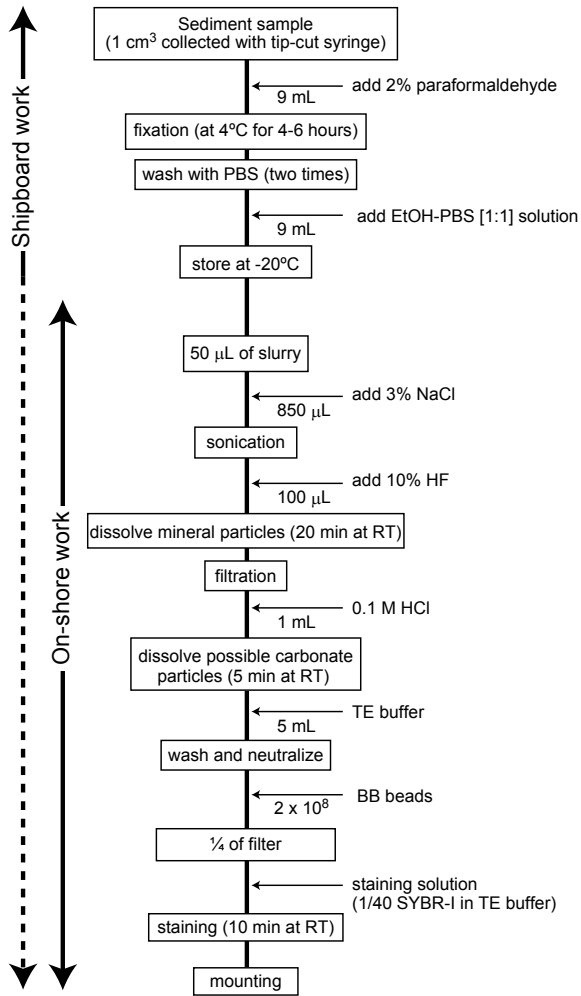


Figure 2. Flow diagram of standard sample preparation protocol. Up to 3.5 x 10⁻³ cm³ of sediment is mounted on the slide

The microscopic imaging is controlled with the software in a “Scan Slide” function that scans a user-defined area of the sample while adjusting the focus on each plane. As the deviation of the slide thickness was comparably large (0.8–1.0 mm), we programmed a wide-focus adjustment macro searching a focus position through a range of 120-µm Z-positions before scanning each slide. After the wide-focus adjustment, the image acquisition sequence with “Scan Slide” proceeds as follows: (i) scan Z-position under 400 nm excitation and 455/50 nm emission filter to focus on BB beads, (ii) fix Z-mortar and acquire bead image, (iii) change excitation to 490 nm and emission to 525/36 nm (green), (iv) acquire cell image, (v) change emission to 605/52 nm (red), and (vi) acquire background image.

The images obtained are analyzed with the macro in the following way. The fluorescence intensity of each pixel in the green image is multiplied by 100 and divided by that of the red image at the same location. The resulting images showing the ratio of the relative intensity of green/red fluorescence were smoothed by median filtering (3 x 3 pixel square), and watershed lines were drawn to separate cells in close proximity to each other. Based on *Escherichia coli* images in control sediments and cellular signals in natural sub-seafloor sediments, we set the threshold value of relative fluorescence at 110 for automatic cell enumeration. Under these threshold conditions, non-specific signals in heat-sterilized sediments as well as on blank filters resulted in a null count. Figure 4 shows the effect of the HF treatment and the image analysis. Counting performed without the modification results in a serious overestimation (100 times higher) of the biomass.

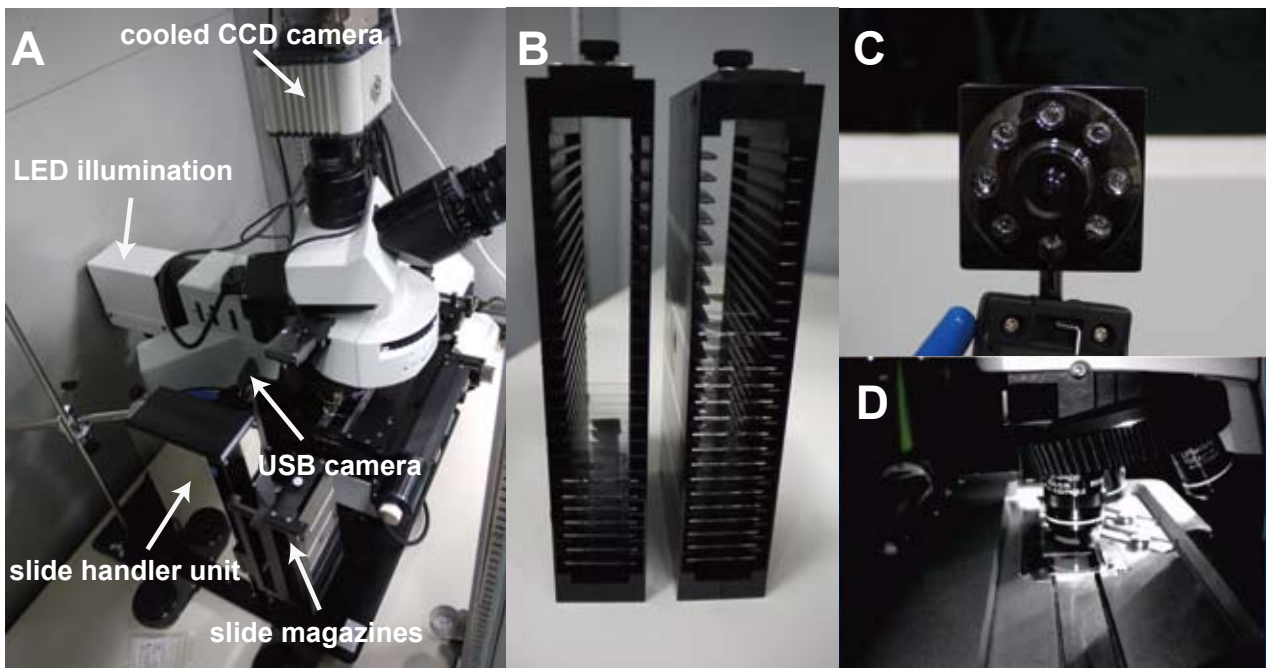


Figure 3. Newly constructed automatic microscopic system with slide handler. [A] Overview of the system. All the units are operated in a dark and cool (15°C) chamber. [B] Slide magazines capable of carrying 25 slides each. [C] USB-connected monitoring camera with infrared LED. [D] The system is monitored without opening the door of the chamber.

Detection Limit of Life Forms and Future Improvement

The lower limit of detection of DNA-containing lifeform signatures (i.e., Archaea, bacteria, and viral components) can only be determined with a maximum load of samples on the filter and a prolonged time for counting. In our examination, $3.5 \times 10^{-3} \text{ cm}^3$ was found to be the maximum load on the filter of 2.5 cm^2 active filtration area. Although we tried to load more on the filter, sediment particles piled up and resulted in focus failure throughout the image field. The maximum load corresponds to $5.1 \times 10^{-5} \text{ cm}^3$ of sediment for a field with a 40x objective lens. According to Kallmeyer et al. (2008), three times more cells are needed in source sediment for detecting at least one cell with 95% probability. The detection limit with one image field is therefore $5.9 \times 10^6 \text{ cells cm}^{-3}$. By considering the time (roughly 8 sec) required for taking one field of image with our system, we can obtain a comparison of detection limit vs. required acquisition time as shown in Table 1. Currently we have already tried and succeeded in analyzing a quarter of the filter and counting down to $3.4 \times 10^3 \text{ cells cm}^{-3}$ in a few hours. To lower the limit further, the required time will increase inversely (Table 1). A practical limit would be less than 100 hours of analysis, which corresponds to a detection limit of $1.3 \times 10^2 \text{ cells cm}^{-3}$. For even lower biomass habitats, a brief centrifugation at $100 \times g$ (Lunau et al., 2005) or a density gradient separation (Kallmeyer et al., 2008) that reduces mineral particles enables larger amounts of sediment to be placed on the filter and extends the detection limit by 10- to 1000-fold. However, the recovery rate depends on natural cell densities and field conditions (Morono et al., 2009) and may sometimes cause serious loss of the cells. The use of a centrifugation step should be carefully considered, and cell concentration should be described as the minimal value in such a case. The system presented here will be useful for primary microbiological onboard data if deployed on scientific drilling platforms. In addition, such a separation technique will open the door for the application of other analytical tools that detect activities of life in low biomass habitats using nanoscale secondary ion mass spectrometry (NanoSIMS; Kuypers and Jørgensen, 2007). Hence, the direction of future technical developments should be towards both the detection of life components with specific signals (e.g., deep UV excitation, see Bhartia et al., 2008) and the detection of activities and metabolic functions of deep seafloor life.

Table 1. Correlation of the lower detection limit and the corresponding time required for obtaining images, amount of sediment, number of images, and number of filters.

Lower limit of detection (cells cm^{-3})	Required time (hrs)	Required sediment volume (cm^3)	Number of image fields	Area of analysis (cm^2)	Number of required filters
1.04×10^4	1	0.000287	450	0.163	1
1.04×10^3	10	0.00287	4,500	1.63	1
1.04×10^2	100	0.0287	45,000	16.3	7
1.04×10^1	1000	0.287	450,000	163	66
1.04	10000	2.87	4,500,000	1630	652

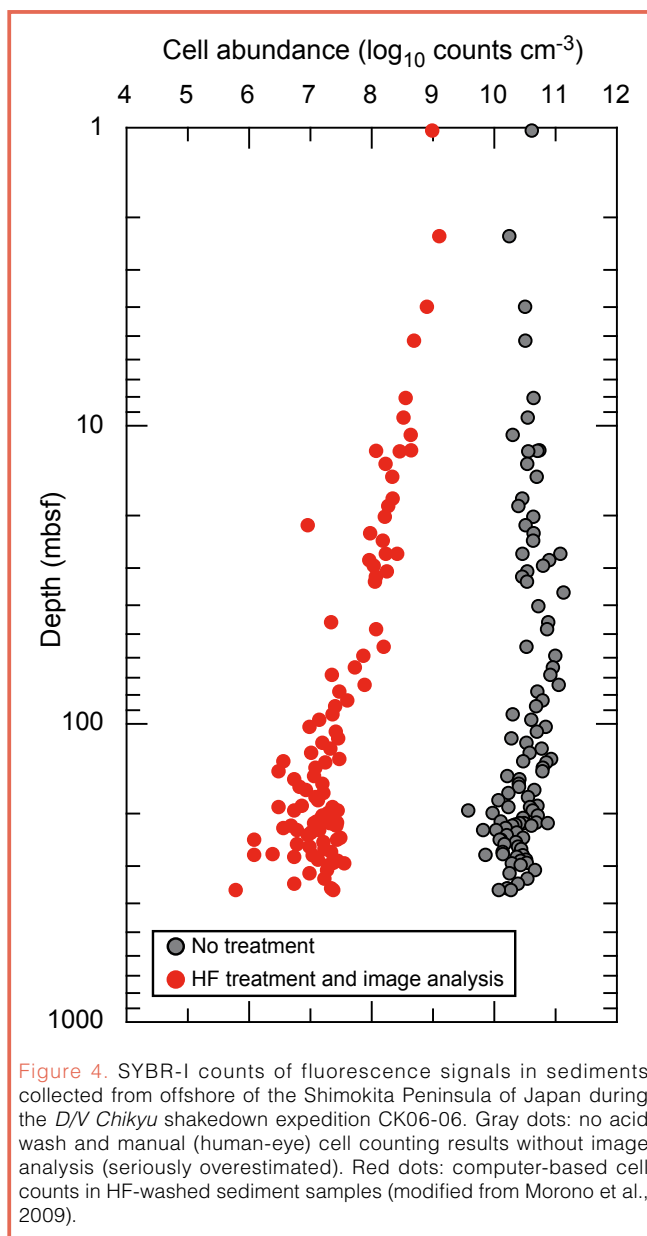


Figure 4. SYBR-I counts of fluorescence signals in sediments collected from offshore of the Shimokita Peninsula of Japan during the *D/V Chikyu* shakedown expedition CK06-06. Gray dots: no acid wash and manual (human-eye) cell counting results without image analysis (seriously overestimated). Red dots: computer-based cell counts in HF-washed sediment samples (modified from Morono et al., 2009).

Acknowledgements

The authors thank Molecular Devices Co. and Olympus Co. for constructing the automated cell counting system and for developing the software macros. We are grateful to the shipboard scientists and crews of the *D/V Chikyu* Shakedown Expedition CK06-06, and the Integrated Ocean Drilling Program (IODP) Expedition 316 for samples and data. The authors are grateful to N. Masui, T. Terada, S. Tanaka, and S.

Fukunaga for filter preparation and technical supports. This study was supported in part by JAMSTEC Multidisciplinary Research Promotion Award 2008 (to YM and FI).

References

- Bhartia, R., Hug, W.F., Salas, E.C., Reid, R.D., Sijapati, K.K., Tsapin, A., Abbey, W., Nealson, K.H., Lane, A.L., and Conrad, P.G., 2008. Classification of organic and biological materials with deep ultraviolet excitation. *Appl. Spect.*, 62:1070–1077, doi:10.1366/000370208786049123.
- Cragg, B.A., Parkes, R.J., Fry, J.C., Weightman, A.J., Maxwell, J.R., Kastner, M., Hovland, M., Whiticar, M.J., Sample, J.C., and Stein, R., 1995. Bacterial profiles in deep sediments of the Santa Barbara Basin, Site 893. *Proc. ODP Sci. Res.*, 146 (Part 2):139–144.
- D'Hondt, S., Inagaki, F., Ferdelman, T., Jørgensen, B.B., Kato, K., Kemp, P., Sobecky, P., Sogin, M., and Takai, K., 2007. Exploring seafloor life with the Integrated Ocean Drilling Program. *Sci. Drill.*, 5:26–37, doi:10.2204/iodp.sd.5.03.2007.
- D'Hondt, S., Jørgensen, B.B., Miller, D.J., Batzke, A., Blake, R., Cragg, B.A., Cypionka, H., Dickens, G.R., Ferdelman, T., Hinrichs, K.-U., Holm, N.G., Mitterer, R., Spivack, A., Wang, G., Bekins, B., Engelen, B., Ford, K., Gettemy, G., Rutherford, S.D., Sass, H., Skilbeck, C.G., Aiello, I.W., Guerin, G., House, C.H., Inagaki, F., Meister, P., Naehr, T., Niitsuma, S., Parkes, R.J., Schippers, A., Smith, D.C., Teske, A., Wiegel, J., Naranjo Padillo, C., and Solis Acosta, J.L., 2004. Distributions of microbial activities in deep seafloor sediments. *Science*, 306:2216–2221, doi:10.1126/science.1101155.
- D'Hondt, S., Rutherford, S., and Spivack, A.J., 2002. Metabolic activity of subsurface life in deep-sea sediments. *Science*, 295:2067–2070, doi:10.1126/science.1064878.
- Engelen, B., Zieglmüller, K., Wolf, L., Köpke, B., Gittel, A., Cypionka, H., Treude, T., Nakagawa, S., Inagaki, F., Lever, M.A., and Steinsbu, B.O., 2008. Fluids from the oceanic crust support microbial activities within the deep biosphere. *Geomicrobiol. J.*, 25:56–66, doi:10.1080/01490450701829006.
- Hoehler, T.M., 2004. Biological energy requirements as quantitative boundary conditions for life in the subsurface. *Geobiology*, 2:205–215, doi:10.1111/j.1472-4677.2004.00033.x.
- Inagaki, F., and Nakagawa, S., 2008. Spatial distribution of the seafloor life: Diversity and biogeography. In Dilek, Y., Furnes, H., and Muehlenbachs, K. (Eds.), *Links Between Geographical Processes, Microbial Activities and Evolution of Life*. New York (Springer Verlag), 135–158.
- Inagaki, F., Nunoura, T., Nakagawa, S., Teske, A., Lever, M., Lauer, A., Suzuki, M., Takai, K., Delwiche, M., Colwell, F.S., Nealson, K.H., Horikoshi, K., D'Hondt, S., and Jørgensen, B.B., 2006. Biogeographical distribution and diversity of microbes in methane hydrate-bearing deep marine sediments on the Pacific Ocean Margin. *Proc. Natl. Acad. Sci. U.S.A.*, 103:2815–2820, doi:10.1073/pnas.0511033103.
- Inagaki, F., Suzuki, M., Takai, K., Oida, H., Sakamoto, T., Aoki, K., Nealson, K.H., and Horikoshi, K., 2003. Microbial communities associated with geological horizons in coastal seafloor sediments from the Sea of Okhotsk. *Appl. Environ. Microbiol.*, 69:7224–7235, doi:10.1128/AEM.69.12.7224-7235.2003.
- Kallmeyer, J., Smith, D.C., Spivack, A.J., and D'Hondt, S., 2008. New cell extraction procedure applied to deep subsurface sediments. *Limnol. Oceanogr. Methods*, 6:236–245.
- Kuypers, M.M.M., and Jørgensen, B.B., 2007. The future of single-cell environmental microbiology. *Environ. Microbiol.*, 9:6–7, doi:10.1111/j.1462-2920.2006.01222_5.x.
- Lunau, M., Lemke, A., Walther, K., Martens-Habbena, W., and Simon, M., 2005. An improved method for counting bacteria from sediments and turbid environments by epifluorescence microscopy. *Environ. Microbiol.*, 7:961–968, doi:10.1111/j.1462-2920.2005.00767.x.
- Morono, Y., Terada, T., Masui, N., and Inagaki, F., 2009. Discriminative detection and enumeration of microbial life in marine subsurface sediments. *ISME J.*, 3:503–511, doi:10.1038/ismej.2009.1.
- Parkes, R.J., Cragg, B.A., and Wellsbury, P., 2000. Recent studies on bacterial populations and processes in seafloor sediments: A review. *Hydrogeol. J.*, 8:11–28, doi:10.1007/PL00010971.
- Roussel, E.G., Bonavita, M.C., Querellou, J., Cragg, B.A., Webster, G., Prieur, D., and Parkes, R.J., 2008. Extending the sub-sea-floor biosphere. *Science*, 320:1046, doi:10.1126/science.1154545.
- Teske, A.P., 2006. Microbial communities of deep marine subsurface sediments: Molecular and cultivation surveys. *Geomicrobiol. J.*, 23:357–368, doi:10.1080/01490450600875613.
- Weinbauer, M.G., Beckmann, C., and Höfle, M.G., 1998. Utility of green fluorescent nucleic acid dyes and aluminum oxide membrane filters for rapid epifluorescence enumeration of soil and sediment bacteria. *Appl. Environ. Microbiol.*, 64:5000–5003.
- Whitman, W.B., Coleman, D.C., and Wiebe, W.J., 1998. Prokaryotes: The unseen majority. *Proc. Natl. Acad. Sci. U.S.A.*, 95:6578–6583, doi:10.1073/pnas.95.12.6578.

Authors

Yuki Morono and Fumio Inagaki, Geomicrobiology Group, Kochi Institute for Core Sample Research (KOCHI), Japan Agency for Marine-Earth Science and Technology (JAMSTEC), Monobe B200, Nankoku, Kochi 783-8502, Japan, e-mail: morono@jamstec.go.jp.

Photo Credits

Fig. 1 and 3: Yuki Morono, JAMSTEC